Neutron single-particle states populated via proton emission from ^{146}Tm and ^{150}Lu

T. N. Ginter,[1,2,3,4,*] J. C. Batchelder,[3] C. R. Bingham,[5,6] C. J. Gross,[6] R. Grzywacz,[5,6,7] J. H. Hamilton,[1] Z. Janas,[7] M. Karny,[5,7] A. Piechaczek,[8] A. V. Ramayya,[1] K. P. Rykaczewski,[6] W. B. Walters,[9] and E. F. Zganjar[8]

[1] *Department of Physics and Astronomy, Vanderbilt University, Nashville, Tennessee 37235, USA*

[2] *Nuclear Science Division, Lawrence Berkeley National Laboratory, Berkeley, California 94720, USA*

[3] *UNIRIB, Oak Ridge Associated Universities, Oak Ridge, Tennessee 37831, USA*

[4] *Joint Institute for Heavy Ion Research, Oak Ridge, Tennessee 37831, USA*

[5] *Department of Physics and Astronomy, University of Tennessee, Knoxville, Tennessee 37996, USA*

[6] *Physics Division, Oak Ridge National Laboratory, Oak Ridge, Tennessee 37831, USA*

[7] *Institute of Experimental Physics, Warsaw University, PL-00681 Warsaw, Hoża 69, Poland*

[8] *Department of Physics and Astronomy, Louisiana State University, Baton Rouge, Louisiana 70803, USA*

[9] *Department of Chemistry, University of Maryland, College Park, Maryland 20742, USA*

(Received 27 May 2003; published 30 September 2003)

Proton emission from the odd-odd nuclei ^{146}Tm and ^{150}Lu has been reinvestigated by means of the recoil mass spectrometer. In the ^{146}Tm study, the strongest proton transitions at 1.12 MeV and at 1.19 MeV have been assigned to the decay of ^{146m}Tm ($T_{1/2}=200\pm10$ ms) and to the ^{146gs}Tm decay ($T_{1/2}=80\pm10$ ms), respectively. Three new proton lines were identified at 0.89 MeV, 0.94 MeV, and 1.01 MeV. The observed decay pattern has been interpreted by using spherical estimates of emission probabilities. The decays of ^{146m,gs}Tm to the $\nu s_{1/2}$ ^{145}Er ground state and to excited neutron states originating from the $\nu h_{11/2}$ orbital are reported. This work represents the first observation of fine structure in proton emission from an odd-odd nucleus. In the ^{150}Lu study, the proton energy and half-life values of $E_p=1277\pm8$ keV and $T_{1/2}=39^{+8}_{-6}$ μs for the decay of ^{150m}Lu were obtained with better precision, but no evidence for fine structure in the proton emission was found.

DOI: 10.1103/PhysRevC.68.034330 PACS number(s): 21.10.Pc, 23.50.+z, 27.60.+j

I. INTRODUCTION

Proton-emission studies provide the best means currently available to explore nuclear structure beyond the proton drip line. In the last decade, the construction of new recoil mass spectrometers together with the development of double-sided silicon strip detectors and advances in signal processing have led to an explosion of work on proton emitters [1–3]. The angular momentum dependence of the proton-emission rate enables the mapping of single-particle proton states through the study of spherical emitters. This dependence even makes it possible to infer the structural composition of proton-emitting states in deformed nuclei [4–10].

The observation of fine structure in the proton-emission from odd-A nuclei has provided another access point to nuclear structure information. Such measurements on $^{131}_{63}Eu_{68}$ [11], $^{141}_{67}Ho_{74}$ [12], and $^{145}_{69}Tm_{76}$ [13] resulted in a more detailed description of the emitting state's wave function (see, e.g., Refs. [9,14]) and allowed the deformation of the nuclear potential to be estimated based on the measured energy of the 2^+ state populated via the proton transition.

In an experiment performed at the Holifield radioactive ion beam facility (HRIBF) at Oak Ridge National Laboratory, we have observed a new instance of fine structure in proton-emission—proton transitions from an odd-odd nucleus ^{146}Tm populating neutron excited levels in its even-Z, odd-N daughter ^{145}Er. This observation extends the application of proton-emission studies to yet another realm of nuclear structure: the probing of neutron single-particle daughter states.

Earlier work on ^{146}Tm [15] had resulted in the identification of two proton transitions: an intense one at 1119 ± 5 keV ($T_{1/2}=235\pm27$ ms) and a weaker one at 1189 ± 5 keV ($T_{1/2}=72\pm23$ ms). Several considerations motivated our reinvestigation of the ^{146}Tm proton decay to search for fine structure. Calculations following the macroscopic-microscopic model presented in Ref. [16] suggested the existence of low-lying (within 250 keV) neutron $s_{1/2}$, $d_{3/2}$, and $h_{11/2}$ states in the daughter nucleus ^{145}Er, thus making the population of such states by proton-emission energetically feasible. As Fig. 1 shows, the experimental level systematics for the less exotic $N=77$ isotones confirm this expectation, indicating the $\nu d_{3/2}$ and $\nu h_{11/2}$ states at about 100–200 keV and 200–300 keV, respectively, above the $\nu s_{1/2}$ ground state. Furthermore, the formation of states in the odd-Z, odd-N parent nucleus by configuration mixing from among the multiple ways single-particle neutron and proton orbitals can couple enhances the prospect that proton-emission can populate some of the expected low-lying excited neutron states.

The reinvestigation of ^{146}Tm was accompanied by an experiment to search for fine structure in the neighboring odd-odd proton-emitter ^{150}Lu. The two proton transitions detected for ^{150}Lu were already assigned in earlier work as originating from the ^{150gs}Lu [17–19] and the ^{150m}Lu decays [19].

II. EXPERIMENTAL PROCEDURES AND RESULTS FOR ^{146}Tm

We produced ^{146}Tm via the $p3n$ reaction channel using a beam of ^{58}Ni on a ^{92}Mo target of thickness 0.91 mg/cm^2.

*Present address: National Superconducting Cyclotron Laboratory, Michigan State University, East Lansing, MI 48824.

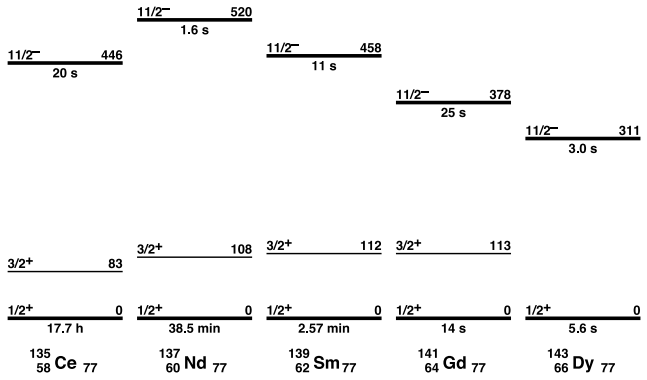

FIG. 1. Synopsis of the experimentally determined level systematics for the lightest even-Z $N=77$ isotones. The level energies are labeled in MeV. The half-lives of $\nu h_{11/2}$ isomeric states are also given.

The beam was delivered at an energy of 292 MeV and with an intensity of 10 particle nA from the HRIBF 25-MV tandem accelerator. The total beam-on-target time was about 72 h.

We used the HRIBF recoil mass spectrometer (RMS) [20] to separate ions recoiling from the target and deliver mass $A=146$ ions for implantation into a double-sided silicon strip detector (DSSD) [21]. To minimize the possibility of losses in the spectrometer, a thin carbon foil was placed 10 cm downstream from the target position at the front of the RMS to reestablish the charge state equilibrium for any recoils reaching the foil that may have decayed by internal conversion [22]. The RMS was set to accept recoils with a central energy of 90 MeV and was run in the converging mass mode to deliver mass 146 recoils in two charge states, 26^+ and 27^+, to the DSSD. Baffles at the focal plane were used to block most recoils from masses other than 146 from reaching the DSSD. The RMS transmission efficiency for this type of reaction is typically about 5%.

A multiwire, gas-filled, position sensitive avalanche counter (PSAC) was used in front of the DSSD at the RMS focal plane. The PSAC not only provided mass identification of the recoils based on their observed positions, but it also distinguished between decay and low energy implantation events in the DSSD by whether or not these events appeared in coincidence with signals from the PSAC.

The 60-μm-thick DSSD covered an area of 4×4 cm^2 and consisted of 40 horizontal and 40 vertical 1-mm-wide strips. This strip arrangement creates 1600 independent pixels identified by position; the time and energy of implanted ions and their subsequent decays by proton or α emission are recorded.

Signals from the DSSD were processed by using analog electronics provided by the University of Edinburgh [23]. This system features Silena analog to digital converters with FERA readout. Use of this setup for observing proton activity at the RMS focal plane—particularly its effectiveness for observing short-lived activities with half-lives down to a few microseconds—has been discussed previously [5,19,24,25].

The energy with which recoils were implanted into the DSSD was either $\sim$20 MeV (shallow implantation) or $\sim$60 MeV (deep implantation) depending on whether or not a 2.3-mg/cm^2-thick Cu foil was used between the PSAC and DSSD to reduce the energy of the recoils. Decay events in which α particles escaped from the surface of the DSSD (and, hence, deposited only part of their energy into the detector) provide the main source of background for the observation of proton emission in the experiment. In the case of shallow implantation, this background peaks near 1 MeV—on top of the proton transitions—as Fig. 2(a) illustrates. In the case of deep implantation, this background peaks at a higher energy and interferes much less with the proton transitions as Fig. 2(b) shows. The background from recoils implanted more deeply shifts to higher energy because the escaping α particles can deposit a larger portion of their energy before they exit the surface of the DSSD.

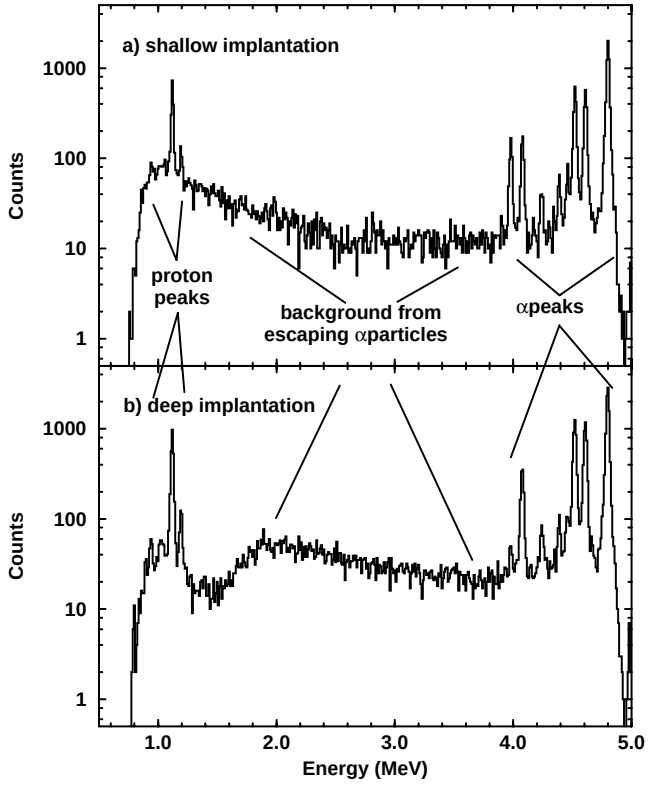

FIG. 2. Mass 146 decay events which follow ions implanted into DSSD pixels within a 1-s time window. A Cu foil is used to reduce the energy with which ions are implanted for the data presented in (a) but not in (b). The α-escape background from shallowly implanted ions masks the proton peaks, while that from deeply implanted ions does not. Differences in the settings of the mass baffles used at the RMS focal plane account for the different patterns of α peaks in the figure.

The overall gain in counts obtained in the two strong proton peaks from this experiment was about an order of magnitude over the previous work [15]. This gain resulted from extending the running time by a factor of 4, doubling the beam current used, and the collection of two charge states of mass 146 at the focal plane.

Figure 3(a) shows the mass 146 decay events observed in

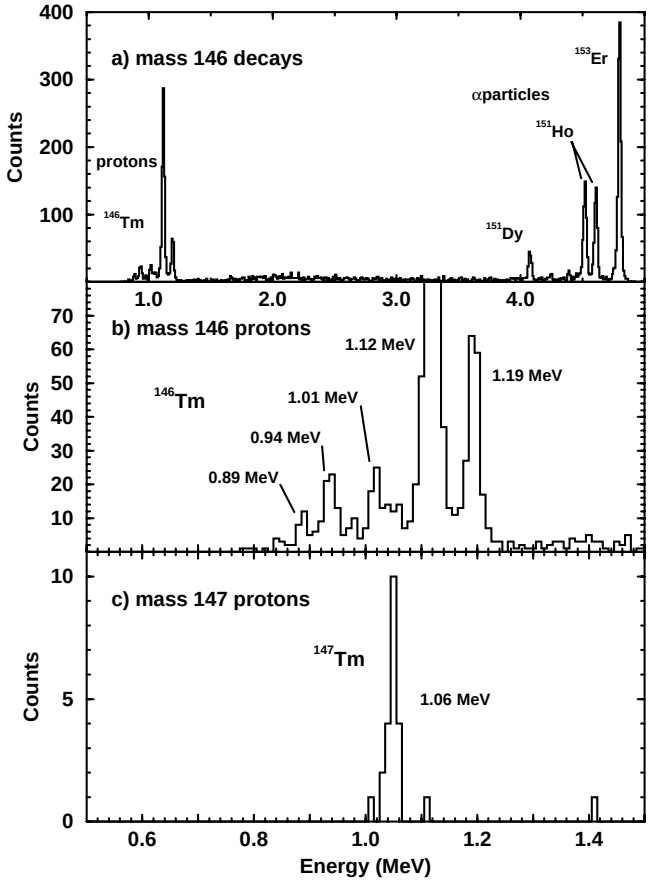

FIG. 3. Data from runs where no Cu foil was used to degrade the energy of the ions implanted into the DSSD (deep implantation). (a) Mass 146 decay events which follow implantation events within a DSSD pixel within a 100-ms time window. The α peaks above 4 MeV result from isotopic impurities in the target. (b) An expanded view of the data from (a) showing the five ^{146}Tm proton transitions. (c) Mass 147 decay events within a 200-ms time window. The $A=146$ and $A=147$ spectra were obtained by gating on the respective mass positions recorded by the PSAC.

the DSSD from the deep implantation data within the first 100 ms after the arrival of a recoil. The peaks above 4 MeV are from the α decay of heavier nuclei. These nuclei originate from isotopic impurities within the target and reach the DSSD because they or their predecessors have mass-to-charge ratios similar to those of the mass 146 recoils.

Figure 3(b) provides an expanded view of the low energy data from Fig. 3(a). In addition to the two previously reported proton lines at 1.12 and 1.19 MeV from ^{146}Tm decay, three new transitions are observed at 0.89, 0.94, and 1.01 MeV. The new peaks appear in both the deep and shallow implantation data. The previous study of ^{146}Tm proton-emission is consistent with our observation of new transitions: there is some evidence of peaklike structures on the background from proton escapes below the strongest 1.12 MeV line (see Fig. 1 of Ref. [15]). Figure 3(c) shows the mass 147 decay events occurring within a time window of 200 ms following the arrival of a recoil at the DSSD. The ^{147}Tm proton line is clearly distinct from the new ^{146}Tm lines. Some contamination from the ^{147}Tm proton transition shows up in the mass 146 decay data because the baffles at the focal plane did not completely block the mass 147 recoils. It is clear that the new transitions arise neither from escape events (proton or α particle) nor from mass 147 contamination.

TABLE I. The energy, half-life, and intensity of proton transitions assigned to the decay of ^{146}Tm. There is no evidence for proton transitions on the microsecond time scale. Background events from randomly correlated escape α particles lead to the large error bars on the present $T_{1/2}$ and intensity measurements. The energy spectra were calibrated using the known 1119-keV ^{146}Tm proton transition and the 4607-keV α line from ^{151}Ho [see Fig. 3(a)].

Energy (keV)	$T_{1/2}$ (ms)[a]	$T_{1/2}$ (ms)[b]	Intensity (counts)[c]
889±10	190±50		110±30
936±10	80±30		215±35
1014±15	110±50		200±80
1119±5 [15]	200±10	235±27	3590±130
1189±5 [15]	80±10	72±23	490±50

[a]Values based on the deep implantation subset of the data.
[b]Values from [15].
[c]Values based on the entire data set, with a 0-400 ms time window for correlation between the recoil implantation and the decay signal.

Table I presents the experimental proton energies, half-lives, and intensities from our study together with previously reported values. Figure 4 displays the level scheme we propose for ^{146}Tm based on the arguments which follow.

III. DISCUSSION OF ^{146}Tm RESULTS

A. Level systematics

It is possible to understand the lowest states in ^{146}Tm and its proton decay daughter ^{145}Er by using an elementary single-particle shell model. For $Z=69$, $N=77$ ^{146}Tm, there are five proton particles above the $Z=64$ subshell and five neutron holes below the $N=82$ shell. In this region of isotopes, the same three single-particle orbitals lie close to the Fermi surface for both protons and neutrons: $s_{1/2}$, $d_{3/2}$, and $h_{11/2}$. Coupled neutron and proton quasiparticles make up the ground state and low-lying metastable states in odd-odd ^{146}Tm. The experimental information on the sequence and energies of the single-particle states from nearby nuclei should indicate the most likely composition of the parent and daughter state wave functions.

Figure 1 presents the experimental level systematics for the neutron-deficient odd-A $N=77$ isotones, which are relevant for understanding the single-neutron structure of even-Z, odd-N ^{145}Er. The configuration with an $s_{1/2}$ neutron outside the even-even core minimizes the total energy and forms the ground state for these nuclei. The stable trend in energies formed by the lowest excited states resulting from the $\nu d_{3/2}$ and $\pi h_{11/2}$ orbitals suggests a similar level structure for ^{145}Er.

A survey of odd-A Tm isotopes in the vicinity of ^{146}Tm indicates the behavior of the active odd-proton orbitals. In

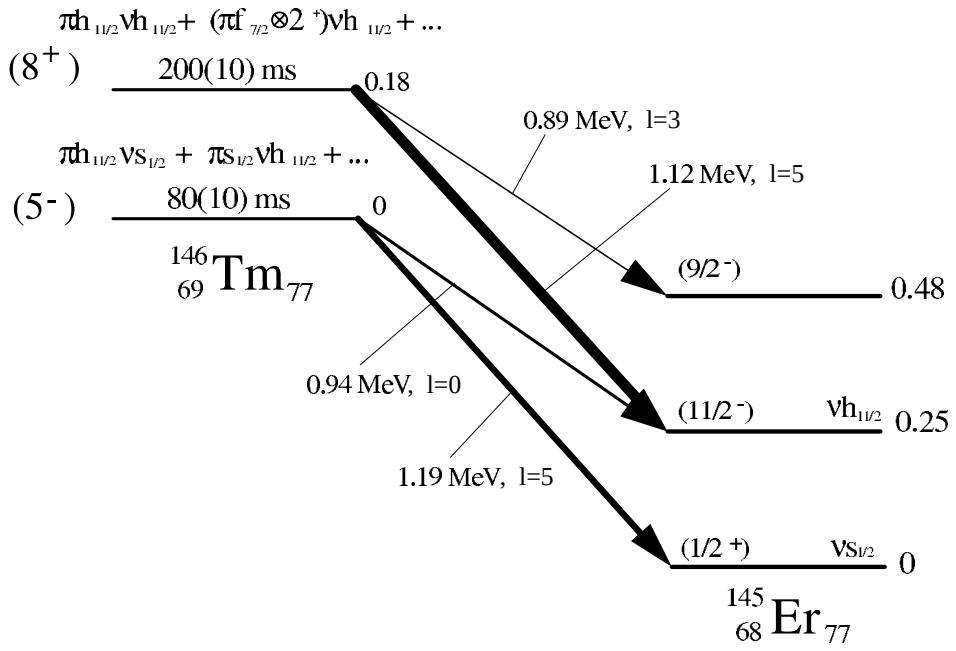

FIG. 4. Partial decay scheme illustrating the proton decay of ^{146gs,m}Tm. The level energies are labeled in MeV. The placement of the 1.01-MeV transition is discussed in the text.

both ^{145}Tm [13,24] and ^{147}Tm [26,27], a dominant $\pi h_{11/2}$ configuration for the lowest energy odd-proton orbital is suggested by the presence of an $h_{11/2}$ proton-emitting level which has been interpreted as the ground state. For ^{147}Tm, decay and in-beam studies [17,18,27] reveal a proton-emitting $d_{3/2}$ excited state at 60 keV; in ^{151}Lu, representing the "^{147}Tm$+\alpha$" system, the proton-emitting $d_{3/2}$ excited state is known at 77 keV above the $\pi h_{11/2}$ ground state [25]. In the heavier Tm isotopes at $N=82$, 84, and 86 (see Fig. 3 in Ref. [25]), an $I^{\pi}=1/2^{+}$ level is observed within 50 keV above the $\pi h_{11/2}$ orbital and has been interpreted as the $\pi s_{1/2}$ state.

The data on nearby even-A Tm isotopes may be used to suggest the quasiparticle configurations to be expected for states in ^{146}Tm. A $\pi h_{11/2}\nu h_{11/2}$ coupling has been attributed to the observed $T_{1/2}=5.2$ ms, $I^{\pi}=10^{+}$ state in ^{150}Tm [28]; a $\pi h_{11/2}\nu s_{1/2}$ coupling is reported for the $T_{1/2}=2.22$ s, $I^{\pi}=6^{-}$ level [29], 671 keV below the 10^{+} state. In the proton unbound (but not proton-emitting) nucleus ^{148}Tm, only the $(9^{+},10^{+},11^{+})$ $\pi h_{11/2}\nu h_{11/2}$ state has been observed [30]—likely because high-spin states are yrast and, thus, are predominantly populated in heavy ion fusion-evaporation reactions. The lower-spin $\pi h_{11/2}\nu s_{1/2}$ state in ^{148}Tm, likely with weaker direct population, was not detected in Ref. [30].

A recent paper [31] on less exotic odd-odd $N=77$ isotones of ^{146}Tm, ^{142}Tb, and ^{144}Ho discusses the states resulting from the $\pi h_{11/2}\nu h_{11/2}$ coupling. These states were observed above the states originating from the coupling of the $h_{11/2}$ proton with the $s_{1/2}$ or $d_{3/2}$ neutron. The $I^{\pi}=(7^{+})$, $\pi h_{11/2}\nu h_{11/2}$ state lies 340 keV above the $I^{\pi}=(5^{-})$ state in ^{142}Tb and 56 keV above the $I^{\pi}=(6^{-})$ state in ^{144}Ho. In both nuclei these two states, of positive and negative parity, are isomeric. The work of Ref. [31] supports large configuration mixing and soft triaxial shapes for these nuclei and is consistent with sudden shape changes anticipated for nuclei in this vicinity [32]. Sudden changes in the level sequences could, in principle, also occur at ^{146}Tm; however, in the interpretation of the present data, we follow the experimental level systematics of the heavier Tm isotopes and the $N=77$ odd-A nuclei.

B. Proton-emission rates and structure of ^{146}Tm states

Table II lists the proton rates expected for different orbitals as calculated, assuming that the protons tunnel through a barrier based on a spherical potential [33]. For the sake of simplicity, we first consider just the relative intensities of the proton lines in calculating possible wave function compositions; we include the β-decay probability later in our final discussion.

TABLE II. The expected proton partial half-lives $T_{1/2}$ corresponding to the observed proton energies for the proton orbitals possibly active in ^{146}Tm. The listed values were calculated using the spherical approach of Ref. [33]. The $T_{1/2}$ estimates include the vacancy factors u^2 of 0.75, 0.79, 0.985, and 0.65 for the orbitals $s_{1/2}$, $d_{3/2}$, $f_{7/2}$, and $h_{11/2}$, respectively.

E_p (keV)	Predicted $T_{1/2}$ (ms)			
	$s_{1/2}$	$d_{3/2}$	$f_{7/2}$	$h_{11/2}$
889	43	360	1900	1100000
936	7.4	62	330	190000
1014	0.54	4.5	23	13000
1119	0.024	0.2	1.0	570
1189	0.0039	0.032	0.16	87

1. The 1.12-MeV and 1.19-MeV proton transitions

The strongest proton transition at 1.12 MeV most likely originates from the decay of the state based on the $\pi h_{11/2}\nu h_{11/2}$ configuration, which would be dominantly populated in the fusion-evaporation reaction forming ^{146}Tm. The observed energy and half-life is consistent with the $\Delta\ell=5$ emission of a $\pi h_{11/2}$ proton. Thus, the spectator $\nu h_{11/2}$ component in the ^{146}Tm state determines the configuration of the level populated in ^{145}Er.

The energy and half-life of the 1.19-MeV line is consistent with a $\Delta\ell=5$ transition, i.e., the $\pi h_{11/2}$ orbital should be strongly present in the ^{146}Tm wave function. An obvious interpretation for this more weakly populated level is the $(5^-,6^-)$ $\pi h_{11/2}\nu s_{1/2}$ state resulting from the coupling of the lowest energy orbitals available. The $\Delta\ell=5$ proton transition from this configuration would populate the $\nu s_{1/2}$ ground state of ^{145}Er. Thus, since we expect ^{146}Tm to preserve the level structure from the heavier Tm isotopes, the 1.19-MeV line represents the ground-state to ground-state decay.

The $\Delta\ell=5$ character of the 1.12- and 1.19-MeV transitions was recognized already in the first observation of ^{146}Tm proton radioactivity within the framework of a simple spherical calculation [15]. A very recent interpretation of the same data within a particle-vibration coupling model also lists the $\pi h_{11/2}$ orbital as the origin of the emitted protons [34]. Neither work, however, deduced the configurations of proton-emitting states, the energy of the isomeric state relative to the ground state, or the proton separation energy of ^{146gs}Tm.

2. New proton transition at 0.94-MeV

The half-life of the new transition at 0.94 MeV matches the value for the 1.19 MeV line. We therefore assign both transitions to the decay of a single 80-ms state in ^{146}Tm.

The energy and angular momentum of the emitted proton strongly influences the probability of tunneling through the barrier. The fact that the two proton transitions are comparable in intensity and yet have a fairly large energy difference (253 keV) indicates a mixed wave function of the parent state—with the energy difference being compensated by a large difference in the proton orbital angular momentum arising from different components of the emitting state. Since the $s_{1/2}$, $d_{3/2}$, and $h_{11/2}$ single particle orbitals have very similar energies for both protons and neutrons, admixtures to the dominant $\pi h_{11/2}\nu s_{1/2}$ component of the wave function for the $(6^-,5^-)$ state are likely. Configurations leading to the same I^π and consistent with the emitted 0.94-MeV proton having a low orbital angular momentum are possible—namely, $\pi s_{1/2}\nu h_{11/2}$ $(\Delta\ell=0)$ and $\pi d_{3/2}\nu h_{11/2}$ $(\Delta\ell=2)$.

Interpreting the 0.94-MeV transition as the emission of a $\Delta\ell=0$ proton requires a small 4% admixture of the $\pi s_{1/2}\nu h_{11/2}$ configuration to the dominating 96% $\pi h_{11/2}\nu s_{1/2}$ component of the ground-state wave function. This interpretation leads to the level scheme shown in Fig. 4 with the 0.94-MeV line populating the same $\nu h_{11/2}$ level as the 1.12-MeV transition. In the $N=77$ isotones, the $I^\pi=11/2^-$ level is the lowest energy state originating from the $\nu h_{11/2}$ orbital.

Interpreting the 0.94-MeV transition as the emission of a $\Delta\ell=2$ proton requires 24% of the $\pi d_{3/2}\nu h_{11/2}$ configuration and 76% of the $\pi h_{11/2}\nu s_{1/2}$ component in the emitter wave function. In fact, the data do not rule out the presence of both admixtures to the $(6^-,5^-)$ state, with both $\Delta\ell=0$ and $\Delta\ell=2$ protons populating the lowest energy level originating from the $\nu h_{11/2}$ orbital in ^{145}Er.

Having the $\pi h_{11/2}\nu s_{1/2}$ component of the 80-ms state replaced by the $\pi h_{11/2}\nu d_{3/2}$ configuration is less likely since the $\nu s_{1/2}$ orbital should be below the $\nu d_{3/2}$ one (see Fig. 1). A small admixture cannot be excluded, however. The resulting $\Delta\ell=5$ proton with a transition energy of $\sim$100–200 keV below the one at 1.19 MeV, see Fig. 1, would populate the excited state originating from the $\nu d_{3/2}$ orbital. The intensity of such a transition is below the sensitivity limit of the present experiment.

3. New proton transition at 0.89 MeV

The observed half-life of the weakest observed proton line at 0.89 MeV suggests that it originates from the $T_{1/2}=200$ ms state. This line can be interpreted as a $\Delta\ell=3$ proton transition resulting from the admixture to the emitter wave function, in which the $\pi f_{7/2}$ orbital coupled to the 2^+ core vibration replaces the $\pi h_{11/2}$ orbital in the $\pi h_{11/2}\nu h_{11/2}$ part of the wave function. A 3–4% admixture of the $\pi f_{7/2}\otimes 2^+$ configuration to the dominant $\pi h_{11/2}\otimes 0^+$ part of the wave function was recently reported for the neighboring proton-emitter ^{145}Tm based on the observation of fine structure in the proton-emission [13,34,35]. The ratio of these ^{145}Tm wave function components varies from 1:8 [34] to 1:18 in the spherical approach presented in Ref. [13]. The intensity ratio of the 0.89-MeV and 1.12-MeV lines can be explained based on a wave function with a $9\pm3\%$ admixture of $[\pi f_{7/2}\otimes 2^+]\nu h_{11/2}$ together with a $[\pi h_{11/2}\otimes 0^+]\nu h_{11/2}$ component of about 90%. The daughter state in ^{145}Er, populated by the 0.89-MeV proton line at an excitation energy of 483 keV, would originate from the $11/2^-$ $\nu h_{11/2}$ bandhead at 250 keV.

4. New proton transition at 1.01 MeV

Because of the uncertainty in the measured half-life of the weak transition at 1.01 MeV, we cannot infer its origin unambiguously. We thus discuss only options for the placement of this transition in the decay scheme shown in Fig. 4.

(1) The 1.01-MeV line originates from the 200-ms $\pi h_{11/2}\nu h_{11/2}$ state. Its small intensity of $\sim 6\pm2\%$ compared to the most intense transition at 1.12 MeV can be understood as arising from the $\Delta\ell=5$ emission to a state associated with the $\nu h_{11/2}$ orbital. Spherical WKB calculations [33] predict $\sim$4% for the intensity ratio of $\Delta\ell=5$ transitions at 1.01 and 1.12-MeV. The transition between $\pi h_{11/2}\nu h_{11/2}$ ^{146m}Tm and a level at 0.36 MeV associated with the $\nu h_{11/2}$ orbital in ^{145}Er is the most likely placement for the 1.01-MeV line.

(2) The 1.01-MeV transition originates from the 80-ms state. A $\Delta\ell=5$ transition from a possible $\pi h_{11/2}\nu d_{3/2}$ component and populating the $\nu d_{3/2}$ state in ^{145}Er can be ruled out because of the strong dependence of the tunneling probability on energy. Scaling from the observed intensity of the

1.19-MeV transition, only about three counts are expected for the 1.01-MeV line even assuming an unrealistically large fraction of 50% for the $\pi h_{11/2}\nu d_{3/2}$ component in the wave function. However, as in the case of the 0.94-MeV transition, the 1.01-MeV line could result from small admixtures of $\pi s_{1/2}\nu h_{11/2}$ or $\pi d_{3/2}\nu h_{11/2}$ to the wave function, and it would populate the $\nu h_{11/2}$ state in ^{145}Er via either a $\Delta\ell=0$ or a $\Delta\ell=2$ transition. For example, the 1.01-MeV line could represent the $\Delta\ell=2$ transition to the lowest $11/2^-$ $\nu h_{11/2}$ state at 175 keV in ^{145}Er, while the $\Delta\ell=0$, 0.94-MeV line populates a $9/2^-$ or second $11/2^-$ level at 253 keV. Such a scenario would require a wave function composition of about 94% $\pi h_{11/2}\nu s_{1/2}$, 2% $\pi d_{3/2}\nu h_{11/2}$, and 4% $\pi s_{1/2}\nu h_{11/2}$ to account for the observed relative intensity ratio of about 5:2:2 for the 1.19, 1.01, and 0.94 MeV lines. If $\Delta\ell=0$ and $\Delta\ell=2$ are assumed for the 1.01- and 0.94-MeV transitions, respectively, the 80-ms state wave function has a 76% $\pi h_{11/2}\nu s_{1/2}$ component deexciting via the 1.19-MeV line, a 0.2% $\pi s_{1/2}\nu h_{11/2}$ component deexciting via the 1.01-MeV line, and a 24% $\pi d_{3/2}\nu h_{11/2}$ component deexciting via the 0.94-MeV line. Note that in this scenario, which requires a possible 175-keV state in ^{145}Er, there would be an additional 1.05-MeV proton transition from the 200-ms ^{146m}Tm to this level. Such a weak 1.05-MeV line cannot be detected in the presented experiment because of the presence of ^{147}Tm contamination.

(3) The 1.01-MeV line originates from a new low-spin positive parity state in ^{146}Tm. Such a state with $I^\pi=1^+$ has been reported in the odd-odd $N=77$ isotones up to ^{142}Tb, but has not been identified so far in the neighboring heavier odd-odd Tm isotopes. A low-spin, positive parity state would result from the coupling of *s* and *d* protons and neutrons with possible spin values of 0, 1, 2, and 3. The decay would be restricted to $\Delta\ell=0$ or $\Delta\ell=2$ proton transitions populating $\nu s_{1/2}$ or $\nu d_{3/2}$ levels in ^{145}Er. The weak intensity of the 1.01-MeV line could be explained by the low direct population of the emitting state in a heavy ion reaction. Its half-life, however, should be in the range from 0.5 ms (pure $\Delta\ell=0$) to about 20 ms—a much longer observed value would not allow for this interpretation.

A more precise determination of the decay pattern for the 1.01-MeV proton line is essential for the interpretation of this transition.

5. Proton-γ coincidences

Proton-γ (p-γ) coincidence data would help to confirm the present decay scheme presented in Fig. 4. It should be noted, however, that the $\nu h_{11/2}$ bandhead in ^{145}Er is most likely a long-lived isomeric state. The 0.9-s β activity assigned to the $11/2^-$ $\nu h_{11/2}$ state in ^{145}Er [36] could actually be the β decay from the 253-keV level in Fig. 4. If so, the only p-γ coincidences available involve the weak proton lines at 0.89 and 1.01 MeV. It is clear that the counting statistics must be increased substantially to observe p-γ events.

6. Spin assignments for ^{146gs,m}Tm

There are two options for the coupling of the $h_{11/2}$ and $s_{1/2}$ nucleons in the ground state of ^{146}Tm: $I^\pi=5^-$ or $I^\pi=6^-$. Our observation of fine structure in the proton-emission from ^{146gs}Tm to the $s_{1/2}$ and $h_{11/2}$ neutron states in ^{145}Er does not differentiate between these options. There is, however, a lack of evidence for a 0.18-MeV isomeric transition between the high-spin ^{146m}Tm and ^{146gs}Tm. A 0.18-MeV $E3$ transition (e.g., between 8^+ and 5^-) in ^{146}Tm would have a long half-life of about 400 ms, while an $M2$ transition (e.g., between 7^+ and 5^-) would be much faster, with a lifetime in the microsecond regime. This fact suggests that a spin difference of at least $\Delta I=3$ exists between the ground and isomeric states. Thus for ^{146gs}Tm and ^{146m}Tm, the I^π options are 5^- and at least 8^+, respectively, or 6^- and at least 9^+.

The $\pi h_{11/2}\nu h_{11/2}$ state for heavier odd-odd Tm isotopes appears to be coupled to $I^\pi=10^+$ [28,30], while $I^\pi=(7^+)$ has been proposed for the $N=77$ isotones ^{142}Tb and ^{144}Ho [31]. The observation of the 1.12 MeV, $\Delta l=5$ proton line, from the $\pi h_{11/2}\nu h_{11/2}$ ^{146m}Tm to the $\nu h_{11/2}$ state, does not distinguish between these possibilities. However, the weaker $\Delta l=3$ transition at 0.89 MeV most likely populates the 0.48-MeV excited state in ^{145}Er with a spin below $11/2^-$. Such states with $I^\pi=7/2^-$ and $9/2^-$ have been detected about 100 to 200 keV above the $\nu h_{11/2}$ bandhead in the $N=77$ odd-mass isotones including neighboring ^{143}Dy [37,38]. The emission of an $f_{7/2}$ proton from the $8^+[\pi f_{7/2}\otimes 2^+]\nu h_{11/2}$ component of ^{146m}Tm can populate a $9/2^-$ state at 0.48 MeV in ^{145}Er. For an initial spin of ^{146m}Tm above $I^\pi=8^+$, the population of a ^{145}Er state with $I>9/2$ would be required. The existence of such a state at 0.48 MeV is not supported by the available level systematics for neighboring nuclei. Higher-spin states, with $I^\pi=13/2^-$ and $I^\pi=15/2^-$ as well as a second $I^\pi=11/2^-$ state, have only been observed about 400 keV and higher above the $\nu h_{11/2}$ bandhead. Therefore, the proposed spin and parity assignments are $I^\pi=(8^+)$ and $I^\pi=(5^-)$, for ^{146m}Tm and ^{146gs}Tm states, respectively.

7. β decay of ^{146gs,m}Tm

Finally, we comment on the β decay of the proton-emitting states. As with the neighboring nuclei, the ^{146}Tm β decay should be governed by the allowed Gamow-Teller (GT) spin-flip transformation of the $h_{11/2}$ proton into an $h_{9/2}$ neutron. Partial β-decay half-lives of around a few hundred milliseconds can be expected—consider, for example, the $T_{1/2}=220$ ms value predicted for ^{146}Tm [39]. Hence, for the longer-lived isomeric state, β decay represents a substantial part of the decay width, while for the shorter-lived ground state, proton-emission dominates. The proposed structure of the lower-spin ^{146}Tm state could be complemented with a $\pi h_{11/2}\nu d_{3/2}$ component which is ''proton-emission inactive'' and therefore does not change the relative proton intensities, but does contribute to the GT β decay. For the higher-spin state, the observed proton-emission rates indicate that the $\pi h_{11/2}$ orbital dominates; thus, the β decay channel may make a significant contribution to the observed half-life.

IV. REINVESTIGATION OF ^{150}Lu DECAY

We have also reinvestigated the decay of the neighboring odd-odd proton-emitter ^{150}Lu to search for evidence of fine

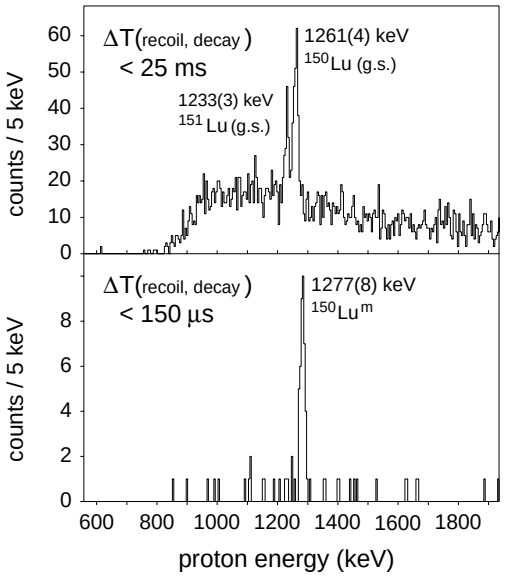

FIG. 5. The energy spectra of proton events collected within 25 ms (upper panel) and 150 μs (lower panel) after the implantation of $A=150$ and $A=151$ recoils into the DSSD.

structure in the proton transitions. The ^{150}Lu nuclei were produced as in our earlier work [19] using a 292-MeV ^{58}Ni beam on a 0.54-mg/cm^2 ^{96}Ru target. As in the ^{146}Tm experiment, a thin charge reset foil was placed 10 cm behind the target to restore the charge state of recoiling ions which may have been altered by isomeric deexcitations involving conversion electrons [20,22]. An observed increase in the yield of ^{150m}Lu proton events compared to our earlier work [19], where no charge reset foil was used, suggests the presence of a few-nanosecond isomeric level on the deexcitation path leading to ^{150m}Lu [22]. The new measurement was performed with two other modifications compared to the previous work [19]: (1) a converging solution for the RMS optics [20] resulted in the collection of ^{150}Lu ions in two charge states instead of one; and (2) less restrictive constraints on the ions reaching the DSSD led to a small fraction of neighboring ^{151gs}Lu activity ($E_p=1233$ keV) showing up in the data.

The results of the new measurement are presented in Fig. 5. Improved counting statistics and a better energy calibration yielded more precise values for the half-life and energy for proton-emission from ^{150m}Lu of $T_{1/2}=39^{+8}_{-6}$ μs and $E_p=1277\pm8$ keV. These remeasured values lead to a spectroscopic factor of $S_p=0.33\pm0.06$, which matches the S_p value of $0.34^{+0.12}_{-0.08}$ obtained for the decay of the $\pi d_{3/2}$ state of neighboring ^{151m}Lu [25]. The new data confirm the postulated $\Delta\ell=2$ character [19] of the proton-emission from ^{150m}Lu.

As Fig. 5 shows, no evidence was obtained for fine structure in the proton-emission from ^{150m,gs}Lu. The proton transitions from both states, ^{150gs}Lu ($\Delta\ell=5$ [17–19]) and ^{150m}Lu ($\Delta\ell=2$ [19]), most likely populate the same daughter state—the $\nu s_{1/2}$ ground state of ^{149}Yb.

V. SUMMARY

We have observed three new transitions in the proton-emission from ^{146}Tm, at 0.89 MeV, 0.94 MeV, and 1.01 MeV, which populate excited states in ^{145}Er. The half-lives of the two previously observed transitions, at 1.12 MeV and 1.19 MeV, were remeasured with better precision to be 200 ± 10 ms and 80 ± 10 ms, respectively.

We have shown that within a basic spherical picture it is possible to understand these transitions both in terms of daughter states based on neutron single-particle orbitals as well as how these orbitals couple with proton single-particle orbitals to form the proton-emitting states in ^{146}Tm. The resulting decay scheme reveals that the 200-ms isomeric level is at 0.18 MeV above the 80-ms ground state of ^{146}Tm. The $[\pi h_{11/2}\otimes 0^+]\nu h_{11/2}$ configuration dominates ($>90\%$) the high-spin (8^+) isomer, while a small admixture ($<10\%$) of the $[\pi f_{7/2}\otimes 2^+]\nu h_{11/2}$ configuration is responsible for the proton-emission fine structure from this state (the 0.89-MeV line). The low-spin (5^-) ground state is primarily composed (90%) of the coupling of the $\pi h_{11/2}$ and the $\nu s_{1/2}$ orbitals, and has a small ''mirror'' admixture (4%) of the $\pi s_{1/2}\nu h_{11/2}$ configuration which is responsible for the proton-emission fine structure (the 0.94-MeV line). Alternatively, the fine structure from this state could also be explained as resulting from the coupling of another positive parity proton orbital $\pi d_{3/2}$ to the same $h_{11/2}$ odd neutron, and would thus require a presence of at least 20% of this component in the wave function. The ''proton inactive'' but β-decaying configuration of $\pi h_{11/2}$ coupled to $\nu d_{3/2}$ is also likely to be present in ^{146gs}Tm wave function. The deduced decay scheme places the $\nu h_{11/2}$ orbital 0.25 MeV above the $\nu s_{1/2}$ ground state of ^{145}Er.

The data on proton-emission from the short-lived ^{150m}Lu were improved. No evidence, however, for fine structure was found.

The observation of fine structure in the proton-emission from ^{146}Tm demonstrates for the first time that a proton radioactivity study can be used to probe the neutron single-particle level structure in the daughter nucleus.

ACKNOWLEDGMENTS

This work was supported by the U. S. DOE under Contract Nos. DE-FG05-88ER40407 (Vanderbilt University), DE-AC05-76OR00033 (UNIRIB), DE-FG02-96ER40983 (University of Tennessee), DE-FG05-87ER40361 (JIHIR), DE-FG02-96ER40978 (Louisiana State University), and DE-FG02-94ER40834 (University of Maryland). UNIRIB is a consortium of universities: the state of Tennessee, Oak Ridge Associated Universities, and Oak Ridge National Laboratory, and is partially supported by them. The Joint Institute for Heavy Ion Research has as member institutions the University of Tennessee, Vanderbilt University, and Oak Ridge National Laboratory; it receives support from the three members. Oak Ridge National Laboratory is managed by UT-Battelle for the U.S. Department of Energy under Contract No. ACS-00OR22725.

[1] P.J. Woods and C.N. Davids, Annu. Rev. Nucl. Part. Sci. **47**, 541 (1997).
[2] *Proton-Emitting Nuclei*, edited by J. C. Batchelder, AIP Conf. Proc. No. 518 (AIP, Melville, NY, 2000).
[3] K. Rykaczewski, Eur. Phys. J. A **15**, 81 (2002).
[4] C.N. Davids *et al.*, Phys. Rev. Lett. **80**, 1849 (1998).
[5] K. Rykaczewski *et al.*, Phys. Rev. C **60**, 011301 (1999).
[6] F. Soramel *et al.*, Phys. Rev. C **63**, 031304R (2001).
[7] S.G. Kadmensky, in ENAM98, *Exotic Nuclei and Atomic Masses*, edited by B. M. Sherrill, D. J. Morrissey, and C. N. Davids, AIP Conf. Proc. **455** (AIP, Woodbury, NY, 1999), p. 672, and references therein.
[8] E. Maglione, L.S. Ferreira, and R.J. Liotta, Phys. Rev. Lett. **81**, 538 (1998).
[9] B. Barmore, A.T. Kruppa, W. Nazarewicz, and T. Vertse, Phys. Rev. C **62**, 054315 (2000).
[10] H. Esbensen and C.N. Davids, Phys. Rev. C **63**, 014315 (2001).
[11] A.A. Sonzogni, C.N. Davids, P.J. Woods, D. Seweryniak, M.P. Carpenter, J.J. Ressler, J. Schwartz, J. Uusitalo, and W.B. Walters, Phys. Rev. Lett. **83**, 1116 (1999).
[12] K.P. Rykaczewski *et al.*, in *Mapping the Triangle*, edited by Ani Aprahamian, Jolie A. Cizewski, Stuart Pittel, and N. Victor Zamfir, AIP Conf. Proc. **638** (AIP, Melville, NY, 2002), p. 149.
[13] M. Karny *et al.*, Phys. Rev. Lett. **90**, 012502 (2003).
[14] A.T. Kruppa, B. Barmore, W. Nazarewicz, and T. Vertse, Phys. Rev. Lett. **84**, 4549 (2000).
[15] K. Livingston, P.J. Woods, T. Davinson, N.J. Davis, S. Hofmann, A.N. James, R.D. Page, P.J. Sellin, and A.C. Shotter, Phys. Lett. B **312**, 46 (1993).
[16] W. Nazarewicz, M.A. Riley, and J.D. Garrett, Nucl. Phys. **A512**, 61 (1990).
[17] S. Hofmann, Y.K. Agarwal, P. Armbruster, F.P. Hessberger, P.O. Larsson, G. Münzenberg, K. Poppensieker, W. Reisdorf, J.R.H. Schneider, and H.J. Schött, in *Proceedings of the 7th International Conference on Atomic Masses and Fundamental Constants, AMCO-7 Darmstadt, 1984*, edited by O. Klepper (THD, Schriftenreiche Wissenschaft und Technik, Darmstadt, 1984), Vol. 26, p. 184.
[18] P.J. Sellin, P.J. Woods, T. Davinson, N.J. Davis, K. Livingston, R.D. Page, A.C. Shotter, S. Hofmann, and A.N. James, Phys. Rev. C **47**, 1933 (1993).
[19] T.N. Ginter *et al.*, Phys. Rev. C **61**, 014308 (1999).
[20] C.J. Gross *et al.*, Nucl. Instrum. Methods Phys. Res. A **450**, 12 (2000).
[21] P.J. Sellin *et al.*, Nucl. Instrum. Methods Phys. Res. A **311**, 217 (1992).
[22] T.M. Cormier, P.M. Stwertka, M. Herman, and N.G. Nicolis, Phys. Rev. C **30**, 1953 (1984).
[23] S.L. Thomas, T. Davinson, and A.C. Shotter, Nucl. Instrum. Methods Phys. Res. A **288**, 212 (1990).
[24] J.C. Batchelder *et al.*, Phys. Rev. C **57**, R1042 (1998).
[25] C.R. Bingham *et al.*, Phys. Rev. C **59**, R2984 (1999).
[26] O. Klepper, T. Batsch, S. Hofmann, R. Kirchner, W. Kurcewicz, W. Reisdorf, E. Roeckl, D. Schardt, and G. Nyman, Z. Phys. A **305**, 125 (1982).
[27] D. Seweryniak *et al.*, Phys. Rev. C **55**, R2137 (1997).
[28] R. Broda, P.J. Daly, J.H. McNeill, Z.W. Grabowski, R.V.F. Janssens, R.D. Lawson, and D.C. Radford, Z. Phys. A **334**, 11 (1989).
[29] A. Gadea *et al.*, Z. Phys. A **355**, 253 (1996).
[30] E. Nolte, S.Z. Gui, G. Colombo, G. Korschinek, and K. Eskola, Z. Phys. A **306**, 223 (1982).
[31] C. Scholey *et al.*, Phys. Rev. C **63**, 034321 (2001).
[32] P. Möller, J.R. Nix, W.D. Myers, and W.J. Swiatecki, At. Data Nucl. Data Tables **59**, 185 (1995).
[33] S. Åberg, P.B. Semmes, and W. Nazarewicz, Phys. Rev. C **56**, 1762 (1997); **58**, 3011 (1998).
[34] C.N. Davids and H. Esbensen, Phys. Rev. C **64**, 034317 (2001).
[35] K.P. Rykaczewski *et al.*, Nucl. Phys. **A682**, 270c (2001).
[36] K.S. Vierinen, J.M. Nitschke, P.A. Wilmarth, R.M. Chasteler, A.A. Shihab-Eldin, R.B. Firestone, K.S. Toth, and Y.A. Akovali, Phys. Rev. C **39**, 1972 (1989).
[37] J.R.B. Oliveira *et al.*, Phys. Rev. C **62**, 064301 (2000).
[38] S.-W. Xu *et al.*, Eur. Phys. J. A **16**, 347 (2003).
[39] P. Möller, J.R. Nix, and K.-L. Kratz, At. Nucl. Data Tables **66**, 131 (1997).